

# High power in Advanced LIGO

**Terra Hardwick**  
for the **LIGO Scientific Collaboration**

Louisiana State University,  
Baton Rouge, LA 70803  
email: [terra.hardwick@ligo.org](mailto:terra.hardwick@ligo.org)

**Abstract.** The LIGO detectors have just completed a successful and exciting observation run. Both facilities are now undergoing upgrades and commissioning, including doubling the circulating power in the interferometer which will increase LIGO's sensitivity above 100 Hz. This paper motivates the power increase and discusses the problems in general that arise with higher power and the progress to date with addressing them. Topics include input power noise coupling, parametric instability, and thermal effects.

**Keywords.** gravitational waves, instrumentation: detectors, instrumentation: adaptive optics

---

## 1. Introduction

On September 14, 2015 LIGO made the first ever detection of gravitational waves. This and the next three detections were of binary black hole systems with component masses between 7.5 - 36 solar masses. On August 17, 2017 LIGO detected gravitational waves from a binary neutron star system for which electromagnetic counterparts were also detected. The final neutron star coalescence occurred outside of LIGO's sensitivity band and several of the black hole mergers were pushing that boundary. Better sensitivity at higher frequencies would result in increased range, higher signal to noise ratio (SNR) for all detections and a greater chance of seeing the full merger and ringdown of more systems. These imply better sky localization, better parameter estimation, better characterization of post-merger activity, and a better understanding of the neutron star equation of state.

During LIGO's first two observing runs (O1, O2), the detector operated with 25 W input power; we plan to double this power for the third observing run scheduled to begin Fall 2018. Increasing the power in the interferometer reduces photon shot noise - currently a limiting noise source - which will increase LIGO's sensitivity in the region above 100 Hz.

High power requires a new laser source scheme designed to integrate into the preexisting LIGO laser layout, provide at least 50 W into the interferometer, and meet low noise requirements. During Fall 2017, this scheme was tested and successfully implemented.

Higher power in the interferometer brings parametric instabilities (PI) and thermal aberrations. While schemes for mitigating these problems were already in place during O2, they must be adapted to the increased power levels.

## 2. Fundamental noise in LIGO detectors

The sensitivity of LIGO is limited by anything that causes differential length motion; the sum of all such noises is the strain sensitivity curve for the detectors. Fundamental noise sources are those for which there is a theoretical limit given LIGO's parameters. They include noises such as quantum fluctuations, thermal motion, and residual gas noise. Quantum noise consists of variation in photon arrival time - shot noise - at higher

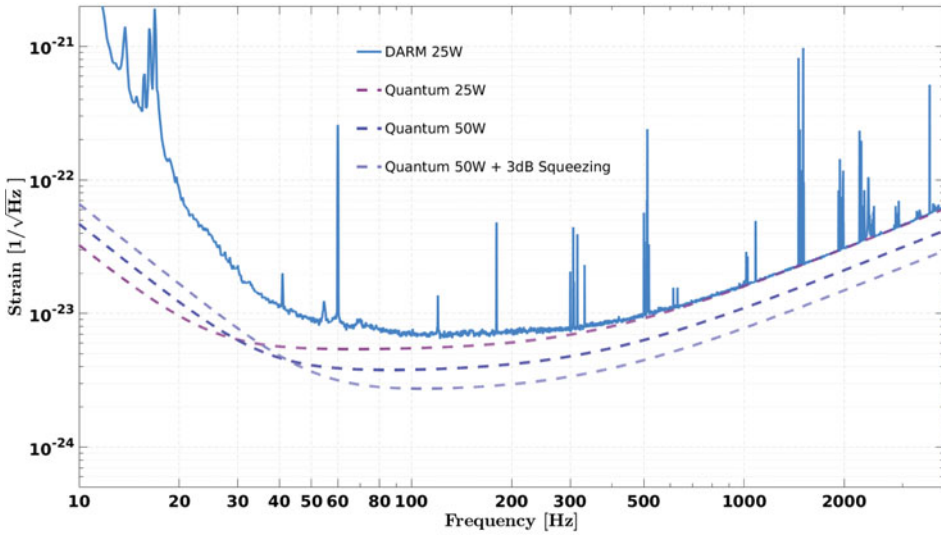


**Figure 1.** Projection of quantum noise with a) 25 W input power, as during O2, b) 50 W input power, and c) 50 W input power + 3dB squeezing, as expected during O3. Shown alongside differential arm (DARM) strain at LIGO Livingston during O2.

frequencies and variation in photon amplitude - radiation pressure - at low frequencies. Saulson (2017)

*Photon shot noise* Fluctuations in photon arrival time result in fluctuations of phase which read out as fluctuations of output power on the photodiode. One can also think of this as sensing noise, or how precisely we are able to measure. This photon shot noise is Poisson in nature, causing power fluctuations of

$$\sigma_{power} = \sqrt{n_{photons}} = \sqrt{\frac{\lambda\tau}{4\pi\hbar c}P} \tag{2.1}$$

where  $\tau$  is the interval over which the number of photons is averaged. In a Michelson interferometer, this fluctuation in power - calibrated in effective strain - has amplitude spectral density

$$h_{shot,FP}(f) = \frac{1}{L}\sqrt{\frac{\hbar c\lambda}{2\pi P}}. \tag{2.2}$$

Note that this is white noise, independent of frequency, but when a full Fabry-Pérot interferometer response is considered, power is frequency dependent. The presence of this photon shot noise puts a fundamental sensitivity limit on strain readout above 100 Hz.

*Radiation pressure* As photons hit the test mass, they exert a force on it, imparting momentum and causing a recoil reaction. Variations in photon arrival time (as discussed above) cause variations in this force:

$$\sigma_{force} = \frac{1}{c}\sigma_{power} \tag{2.3}$$

This can also be thought about as variation in photon amplitude. The fluctuations in force variable move the test mass, injecting noise into the final length readout. This

radiation pressure noise has amplitude spectral density

$$h_{rp}(f) = \frac{1}{mL f^2} \sqrt{\frac{\hbar P_{in}}{2\pi^3 c \lambda}}. \quad (2.4)$$

Note that this is frequency dependent, where the slope is set by the pendulum response of the test mass suspension ( $1/f^2$ ). Radiation pressure puts a fundamental sensitivity limit on strain readout below 100 Hz.

### 3. Reducing quantum noise

Radiation pressure noise and shot noise can be considered together as one frequency-dependent quantum noise source:

$$h_q(f) = \sqrt{h_{shot}^2(f) + h_{rp}^2(f)}. \quad (3.1)$$

Note that at low frequencies, the  $1/f^2$  dependent radiation pressure will dominate, but will be less significant than white shot noise as higher frequencies.

There are two ways to influence quantum noise: squeezing (in amplitude or phase) and changing input power. Squeezing in phase and increasing power will lower LIGO's noise above 100 Hz, giving the desired frequency sensitivity previously discussed. Both techniques add noise at lower frequencies, but currently the LIGO detectors have noise sources (i.e. angular controls and seismic) that are higher than radiation pressure noise so neither scheme will reduce sensitivity at low frequency.

*Squeezing* Radiation pressure noise and shot noise are most fundamentally explained by quantum vacuum fluctuation. These vacuum fluctuations have an amplitude and phase relationship:

$$\sigma_{amp} \sigma_{phase} \geq \frac{\hbar}{2} \quad (3.2)$$

such that there is a limit on the combined decrease of amplitude and phase noise. The quantum noise floor is where  $\sigma_{amp} \sigma_{phase} = \frac{\hbar}{2}$ ; the combined fluctuations of amplitude and phase are as low as possible. Squeezing works on the principle that either can be reduced at the cost of raising the other: phase noise (shot noise) can be lowered if amplitude noise (radiation pressure noise) is raised and vice versa.

To accomplish this, LIGO plans to inject squeezed light into the interferometer. Since LIGO is currently limited by only quantum shot noise at high frequency, phase squeezing will be implemented for the next observing run. While this will subsequently increase amplitude fluctuations, the increased low frequency quantum noise will still sit below other limiting noise factors. Eventually frequency dependent squeezing will be implemented, injecting phase squeezed light at high frequencies and amplitude squeezed light at low frequencies.

*Increased power* Strain optical gain (unit Watts) is how differential arm strain converts to power on the output photo diode.

$$\text{strain optical gain} := \frac{dP_{out}}{dh} = \frac{8\pi}{c} \phi_0 g_\phi f P_{in} \quad (3.3)$$

where  $\phi_0$  is frequency offset from full dark. From this we see that optical gain scales linearly with input power: the higher  $P_{in}$ , the greater change in  $P_{out}$  for differential arm length change. From eq. 2.1, shot noise SNR scales only with the square root of power. Put another way, the fractional fluctuation in number of photons arriving at a test mass

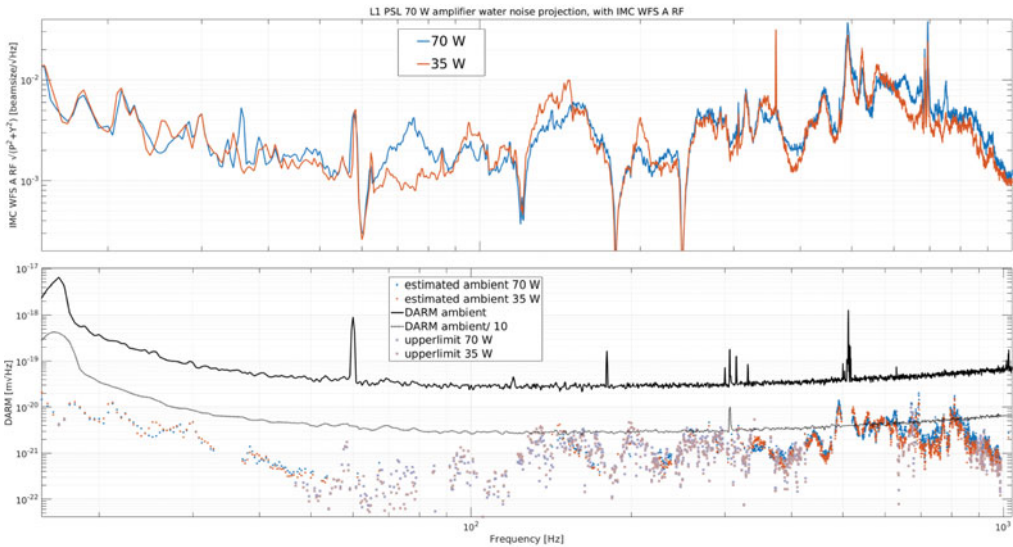


**Figure 2.** Noise projections of table-motion jitter from previous (orange) and new (blue) laser set ups. First, coupling functions are made by injecting noise until a response is seen in DARM (in this case, shaking the optic table). That function can then be multiplied by ambient noise to estimate how far below DARM the nominal noise sits. If the original injection was not strong enough to couple into DARM, only upper limits can be placed.

in some time  $\tau$  is

$$\frac{\sigma_{power}}{power} = \frac{\sqrt{n_{photons}}}{n_{photons}}. \tag{3.4}$$

Thus, increasing power (number of photons) will grow optical gain faster than shot noise, so shot noise strain decreases with greater power:  $h_{shot} \propto \sqrt{1/P}$  (eq. 2.2).

During the first two observing runs, Advanced LIGO ran with 25 W input power. We will double the power during the next run; the expected quantum noise response is shown in fig. 1.

### 4. 70 W amplifier

The 25 W input power of the previous observing run was the maximum power available from the laser configuration at that time. To double this power, a solid-state amplifier has been installed capable of amplifying to over 70 W of optical power with 4 crystals pumped by fiber-coupled diode lasers. Produced by neoLASE, this 70 W amplifier was specifically designed for minimum-impact integration into the previous table set-up and for quiet operation.

The original Advanced LIGO high power plan was to use a high power oscillator capable of producing 200 W output. During the last observing run, this oscillator was found to inject noise into the interferometer through beam pointing and size jitter. Noise originates from the water system cooling the oscillator crystals; water flow is necessarily turbulent for efficient cooling. Water, brought in from removed chillers, is directed via a breakout manifold under the table and travels to the oscillator in tubes along the optic table. Water flows in a closed loop directly over the oscillator crystals in series with auxiliary cooled dumps, etc. Water motion couples into the beam in two ways:

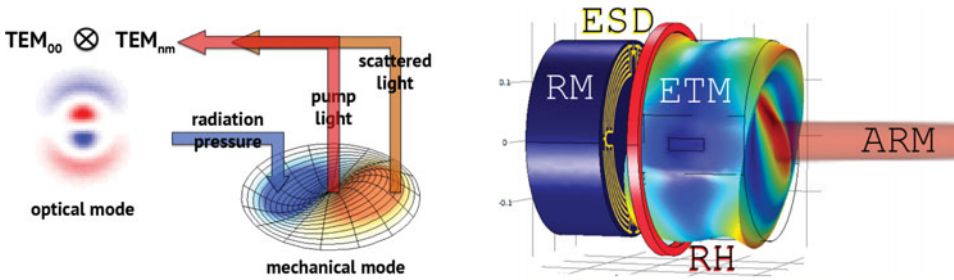


**Figure 3.** Left: Parametric instability (PI) feedback loop: mechanical motion of the test mass can scatter light into a higher order optical mode which then puts radiation pressure back on the optic, reinforcing the mechanical motion. Right: PI damping components: a) the ring heater (RH) circles the test mass towards the back, altering the radius of curvature and thus the optical mode spacing of the arm cavity b) the electrostatic drive (ESD) on the face of the reaction mass (RM) actuates against the back of the test mass with quadrature control, damping the mechanical modes of the test mass..

- turbulent water flow over the crystals couples directly into the beam
- water flow shaking the optics table couples into optics and thus indirectly into the beam

The 70 W amplifier was designed with minimal water flow needs in mind. It will allow LIGO to double input power for the next run but the more modest (if immediate) power goal allows for the full system to have lower flow requirements. The crystals are cooled indirectly and the system is designed in parallel such that the highest water flow needs no longer dictate the flow rate for all water tubes. Since installation, the 70 W amplifier has proven to output stable power over 70 W and jitter noise from table motion is comparable to that from the previous lower power laser set-up; noise projection is still a factor of 2 below DARM at the worst coupling frequency (fig. 2).

### 5. Parametric instability

A main problem that arises as LIGO increases power is the growth of parametric instabilities (PI). Long theorized (see Braginsky (2001)), these instabilities were first observed with 12 W input power and will become more problematic with each increase in power. PI have been successfully mitigated during the previous two observing runs, but increased power will require fine tuning of these mitigation schemes.

*PI overview* Parametric instabilities are run-away mechanisms where the mechanical motion of an arm mirror (test mass) resonance scatters light into a higher-order optical mode in the arm cavity which in turn applies radiation pressure back onto the test mass such that its mechanical motion is reinforced, as shown in Fig. 3.

More specifically, PI can occur when a mechanical mode of an optic falls within the line width of the beat between the carrier and a higher order optical mode (HOM) present in the cavity:

$$f_{mechanical} \sim (p)FSR + (2m + n)TMS \tag{5.1}$$

where  $p, n, m \in \mathcal{N}$ ,  $FSR = \text{free spectral range} = \frac{c}{2L} = 37.5 \text{ kHz}$ , and  $TMS = \text{transverse mode spacing} \approx 5.1 \text{ kHz}$ ,  $\nu_0 = \frac{\pi c}{L}$ . If this mechanical mode gets rung up (perhaps by some thermal excitation), the oscillating mirror surface will scatter light, effectively modulating the 0,0 mode by  $f_{acoustic}$ :

$$f_{mod} = f_{0,0} - f_{acoustic} = f_{0,0} - [(p)FSR + (2m + n)TMS] = f_{HOM} \tag{5.2}$$

since TMS is defined as the frequency spacing between 0,0 and HOM, and FSR simply allows for cavity wrapping.

Once 0,0 and HOM are both present in the cavity, the resulting total field applies radiation pressure back on the surface of the optic, closing the loop; if the transverse amplitude distribution of this field overlaps the spacial surface profile of the original acoustic mode, the radiation pressure reinforces the surface motion resulting in an instability which can grow beyond the limits of the cavity control loops.

If we model this mechanism as a classic feedback loop, as shown by Evans (2010), the gain of the loop for a particular mechanical mode  $m$  is

$$R_m = \frac{8\pi Q_m P}{M\omega_m^2 c\lambda_0} \sum_{n=1}^{inf} \Re[G_n] B_{m,n}^2 \tag{5.3}$$

where  $Q_m$  is the quality factor of the mechanical mode,  $P$  is the circulating power,  $M$  is the mass of the optic,  $\omega_m$  is the mechanical frequency,  $G$  is the optical transfer function, and  $B$  is a term related to the spacial overlap. Note the linear dependence on power.

*Controlling PI* There are two approaches to mitigating parametric instability:

- Changing the optical gain  $G_n$

Since the light scattered at the mechanical mode frequency into the cavity will only resonant if the frequency is within the line width of the transverse mode spacing, tuning the TMS can decrease this frequency overlap, effectively lowering the loop gain (see Zhao (2005), Gras (2010)). Since

$$TMS = \frac{\nu_0}{\pi} \cos^{-1} \sqrt{(1 - L/R_1)(1 - L/R_2)}, \tag{5.4}$$

where  $R_{1,2}$  are the radii of curvature of each optic, altering either optic’s radius of curvature allows us to tune the optical mode spacing. To do this, LIGO uses ring heaters, annular heating elements that radiate heat onto the outer edge of the test mass; changing the temperature difference across the test mass changes its radius of curvature.

- Changing the quality factor  $Q_m$  of the optic

The motion of the test mass can be damped using electrostatic drives (ESD) already in place for low noise actuation (Blair (2017)). Behind each test mass is a reaction mass, whose face has pairs of gold conductors such that a differential voltage can be applied. This puts an electrostatic force on the test mass which couples to the mechanical mode with some coefficient  $b_m$ :

$$F_{ESD,m} = b_m A_q \frac{1}{2} (\Delta V)^2 \tag{5.5}$$

There are 4 independent electrostatic drives on each reaction mass, allowing for quadrature longitudinal actuation; by driving equally and oppositely at the mechanical mode frequency in a pattern that roughly matches it’s surface profile, the mechanical motion can be damped, reducing the parametric gain below unity to bring the loop back to the stable regime (Miller (2011)).

Both methods have been successfully used to mitigate PIs at both LIGO detectors. However, the first method of tuning to a ‘safe zone’ of low parametric gain will become obsolete as power is increased: as the parametric gain increases for all mechanical modes linearly with power, areas of previously low gain to which the optical spacing could be tuned before will no longer exist. Additionally, during power up, the temperature differential across the test mass changes, sweeping the optical mode in a short amount of time, leading to large and fast changes in parametric gain. Additionally, mechanical

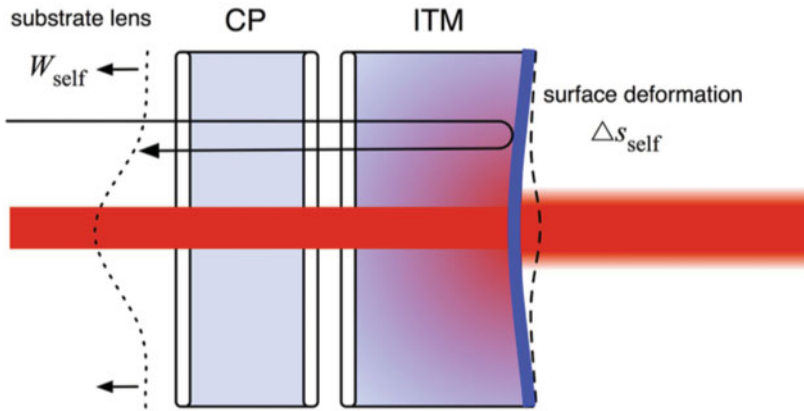


**Figure 4.** Surface deformation and substrate lensing due to self heating. Here the initial test mass (ITM) forming one of the 4 km arm cavities is shown, with the blue line indicating the HR surface. Before the ITM hangs the compensation plate (CP), an identical mass sitting between the ITM and the other coupled cavities of the interferometer.

mode frequencies are proportional to Young's modulus  $E$ ,

$$f_m = A_m \sqrt{E} \Rightarrow \frac{df_m}{dT} = \frac{A_m}{2\sqrt{E}} \frac{dE}{dT} \quad (5.6)$$

so as the optic heats up and as ambient temperatures fluctuate over long lock stretches, the mechanical modes shift in frequency.

## 6. Thermal effects

High power brings thermal consequences: as optics heat up, thermo-optical distortion occurs (see Brooks (2016)). This is especially relevant in the 4 km arm cavities, where there is large power buildup. Thermal distortion affects mode matching between the coupled cavities of the interferometer, resulting in power losses, control instabilities, and increased noise.

The optics that form the arm cavities have nominal coating absorption of 0.5 ppm. As power in the arms is increased to hundreds of kW, the power absorbed will increase to hundreds of mW. The subsequent temperature differential results in surface deformation of the high-reflectivity side of the test masses and substrate lensing due to the change in index of refraction with temperature of the initial test masses of the arms, as shown in fig. 4. These effects distort the wavefronts of the fields in the interferometer, resulting in poor mode matching.

### *Thermal compensation system*

A thermal compensation system was developed to sense and correct thermally-induced distortions. The system includes:

- Ring heaters

Ring heaters provide deformation of the radius of curvature of the test mass counter to that from self heating. The arm cavity beam, roughly centered on the test mass, heats the center of the optic, effectively increasing the radius of curvature; the ring heater, in contrast, heats the outer radius of the optic, effectively decreasing the radius of curvature. Ring heaters have large thermal time constants so are tuned for the steady state operation of the locked interferometer.

- CO<sub>2</sub> lasers

One more degree of control is necessary for mode matching. CO<sub>2</sub> lasers are projected onto the back of the compensation plate (CP), creating a tunable lens between the arm cavities and the other cavities of the interferometer. Before impinging on the CP, the beam passes through a mask that sets a spacial distribution; this mask can be interchanged, allowing for tunable beam shape. The nominal design consists of central heating and annular heating, the former to counteract strong arm cavity central heating transients during locklosses and the latter to tune the residual distortion from the combined ring heater and central heating settings.

All concepts are illustrated together in fig. 4.

## 7. Conclusion

Higher power during the next observing run will give LIGO better sensitivity at high frequency by decreasing shot noise, resulting in higher SNR for gravitational wave detections over a larger frequency band. The increase of power will come from a newly installed, quiet 70 W amplifier and will correspond with squeezer installation. With a power increase comes parametric instabilities and thermal detuning. Control schemes have been developed and successfully tested for avoiding and actively damping PI. Hardware is in place to counteract thermal effects and is being commissioned for the higher power requirements.

## References

- Saulson, P. *Fundamentals of Interferometric Gravitational Wave Detectors*. World Scientific Publishing Co. 2017.
- Braginsky, V. B., Strigin, S. E., & Vyatchanin, S. P. 2001, *Phys. Lett.* A287, 331-338
- Zhao, C., *et al.* 2005, *Phys. Rev. Lett.* 94, 121102
- Blair, C., *et al.* 2017, *Phys. Rev. Lett.* 118, 151102
- Gras S., *et al.* 2010, *Classical and Quantum Gravity* 27, 20
- Evans, M., Barsotti, L., & Fritschel, P. 2010, *Phys. Lett.* A374, 665-671
- Miller, J. 2011, *Phys. Lett.* A375, 788-794
- Brooks, A., *et al.* 2016, *Appl. Opt.* 55, 8256-8265
- Brooks, A., Kelly, T., Veitch, P., & Munch, J. 2007, *Opt. Express* 15, 10370-10375